
Proxy-Free GFlowNet

Ruishuo Chen*
School of Mathematics
Nanjing University
Nanjing, China

Xun Wang
IIS
Tsinghua University
Beijing, China

Rui Hu
IIS
Tsinghua University
Beijing, China

Zhuoran Li
IIS
Tsinghua University
Beijing, China

Longbo Huang†
IIS
Tsinghua University
Beijing, China

Abstract

Generative Flow Networks (GFlowNets) are a promising class of generative models designed to sample diverse, high-reward structures by modeling distributions over compositional objects. In many real-world applications, obtaining the reward function for such objects is expensive, time-consuming, or requires human input, making it necessary to train GFlowNets from historical datasets. Most existing methods adopt a model-based approach, learning a proxy model from the dataset to approximate the reward function. However, this strategy inherently ties the quality of the learned policy to the accuracy of the proxy, introducing additional complexity and uncertainty into the training process. To overcome these limitations, we propose **Trajectory-Distilled GFlowNet (TD-GFN)**, a *proxy-free* training framework that eliminates the need for out-of-dataset reward queries. Our method is motivated by the key observation that different edges in the associated directed acyclic graph (DAG) contribute unequally to effective policy learning. TD-GFN leverages inverse reinforcement learning to estimate edge-level rewards from the offline dataset, which are then used to ingeniously prune the DAG and guide backward trajectory sampling during training. This approach directs the policy toward high-reward regions while reducing the complexity of model fitting. Empirical results across multiple tasks show that TD-GFN trains both efficiently and reliably, significantly outperforming existing baselines in convergence speed and sample quality.

1 Introduction

Generative Flow Networks (GFlowNets or GFNs) [1, 2] are generative models designed to sample compositional objects in proportion to their positive rewards, and have shown strong empirical success across diverse domains including molecule discovery [1], biological sequence design [3], combinatorial optimization [4], fine-tuning of large language models [5] and diffusion models [6].

Despite the promising potential of GFlowNets, interacting with the environment to obtain reward feedback for policy updates is often impractical or infeasible in real-world applications—such as biological and chemical tasks involving costly experiments or simulations, or tasks requiring human evaluation [7]. As a result, learning GFlowNets from historically collected datasets becomes essential.

Current approaches typically adopt a model-based strategy, wherein a proxy model is trained on the dataset to approximate the reward signal from the environment for updating the policy [1, 3, 8–10].

*This work was done during a visit to IIS, Tsinghua University.

†Corresponding author. Correspondence to: longbohuang@tsinghua.edu.cn

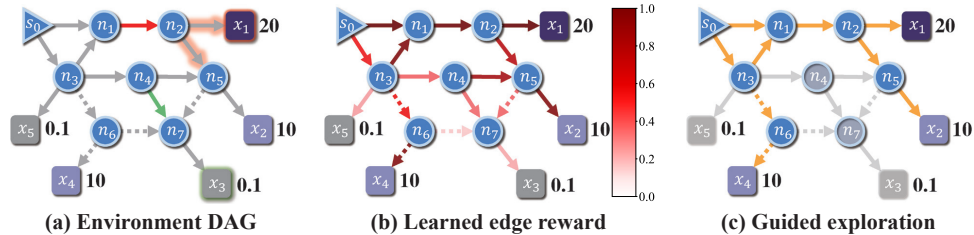


Figure 1: Illustration of our motivation. All subfigures depict an environment DAG, where solid edges represent transitions observed in the dataset and dashed edges indicate unobserved transitions. Reward values are annotated next to the terminal states. (a) Different edges contribute unequally to the final learned distribution. (b) Edge contributions as inferred by TD-GFN. (c) Selective exploration guided by the learned edge contributions.

However, reliance on such proxy reward models imposes a fundamental limitation on the performance of the learned policies, as their effectiveness is inherently constrained by the accuracy of the reward approximation. Inaccuracies or biases in the proxy model inevitably propagate through the learning pipeline, potentially resulting in suboptimal or misleading policies [11–13]. This challenge is particularly pronounced in domains such as language modeling [14, 15], recommendation systems [16], and autonomous driving [17], where surrogate reward models often struggle to generalize beyond the distribution of their training data. Furthermore, constructing a high-quality reward model typically demands a large and diverse dataset, along with substantial domain-specific expertise—both of which are resource-intensive [18–20]. Consequently, dependence on proxy reward models introduces considerable burden, complexity, and uncertainty into the training process, ultimately undermining the reliability and scalability of the overall algorithm.

The limitations of existing training methods naturally give rise to the following question:

Can we train GFlowNets effectively and efficiently without a proxy reward model?

The absence of a proxy reward model implies that out-of-distribution feedback is unavailable during training—posing a significant challenge for GFlowNets, whose objectives inherently require broad coverage of the state space. Consequently, an effective training framework must fully leverage the available historical data, while also generalizing strategically to sufficiently broad unseen regions of the state space, in order to achieve a stronger balance between exploration and exploitation.

Several recent efforts have attempted to address this challenge. An early approach [21] uses offline action probabilities to constrain the learned policy, while COFlowNet [22] penalizes flow on unseen edges to limit policy coverage to dataset-adjacent regions. Both methods aim to improve policy reliability by imposing coarse constraints that merely align policy behavior or coverage more closely with the dataset. However, such constraints impose blunt limitations that hinder generalization beyond the dataset and make performance highly sensitive to data quality and coverage, as they fail to fully exploit the trajectory-level information contained in the dataset. Additionally, [23] explores an “offline” setting with backward sampling from terminal states, but primarily focuses on evaluating sampling strategies rather than proposing a concrete training framework.

To address these challenges, we begin with a key insight: different edges in the environment’s directed acyclic graph (DAG) contribute *unequally* to effective GFlowNet training. As shown in Figure 1(a), removing the red edge ($n_1 \rightarrow n_2$) blocks access to a terminal node with reward 20, while removing the green edge ($n_4 \rightarrow n_7$) only affects a low-reward node (0.1). This disparity underscores the varying importance of edges in learning the target distribution (Figure 1(b)), which can in turn be leveraged to guide the policy in selectively exploring unseen regions (Figure 1(c)).

Motivated by this insight, we propose a novel *proxy-free* GFlowNet training framework, **Trajectory-Distilled GFlowNet (TD-GFN)**, which eliminates reliance on proxy models by avoiding out-of-distribution reward queries. Unlike prior methods that primarily differentiate behaviors based on their proximity to the dataset, TD-GFN provides more informative supervision by capturing the varying importance of transitions across the environment DAG, thereby enabling a more effective exploration–exploitation trade-off.

Specifically, TD-GFN introduces a novel *edge reward function* that quantifies the contribution of each transition in the environment DAG. This function is inferred via inverse reinforcement learning (IRL) from a carefully rebalanced offline dataset, leveraging the theoretical equivalence between GFlowNet training and entropy-regularized reinforcement learning (RL) [24]. The structured supervision provided by the resulting edge rewards enables the policy to generalize strategically beyond observed trajectories, rather than remain confined to dataset-supported regions.

To mitigate the sensitivity to function approximation errors introduced by directly incorporating edge rewards into the training objective—an issue analogous to the limitations observed with proxy reward models—we propose two indirect mechanisms for shaping the GFlowNet policy. First, we prune the environment DAG by removing low-utility transitions as determined by the learned edge rewards. This yields a more compact yet expressive action space that prioritizes structurally informative and high-reward trajectories, while reducing the complexity of model fitting. Second, we introduce a prioritized backward sampling procedure over the pruned DAG, which reinforces the core inductive bias of GFlowNets—allocating attention in proportion to reward—while improving training efficiency by focusing updates on high-value regions of the state space.

Equipped with these novel components, TD-GFN exhibits strong empirical performance across diverse benchmark tasks. Compared to a broad range of baselines, including proxy-based GFlowNet training paradigms, TD-GFN consistently achieves superior performance and faster convergence, underscoring its potential as a more stable and reliable alternative for efficient GFlowNet training.

In summary, we introduce **Trajectory-Distilled GFlowNet (TD-GFN)**, a novel proxy-free training framework that eliminates the need for proxy reward queries on out-of-distribution objects by extracting structural supervision from existing data. The key contributions of TD-GFN are as follows:

- TD-GFN employs inverse reinforcement learning to infer edge-level rewards from a rebalanced offline dataset, capturing the relative importance of transitions within the environment DAG. These edge rewards provide structured, transition-level supervision that enables the policy to generalize beyond the dataset while remaining grounded in reliable behavior.
- Leveraging the inferred edge rewards, TD-GFN prunes low-utility transitions from the environment DAG and introduces a prioritized backward sampling procedure guided by both edge and terminal rewards. This approach concentrates learning on informative regions of the state space and enhances training efficiency by reducing the complexity of model fitting.
- TD-GFN consistently demonstrates strong empirical performance across diverse benchmark tasks, outperforming a wide range of baselines in both convergence speed and final policy quality. These results highlight its effectiveness as a stable and efficient training paradigm within the GFlowNet framework.

2 Preliminaries

In this section, we describe Generative Flow Networks (GFlowNets or GFNs) [1, 2] and the maximum causal entropy inverse reinforcement learning (IRL) framework [25, 26], which help clarify our proposed method. Additional related works are provided in Appendix B for completeness.

2.1 GFlowNets

GFlowNets are defined within an environment represented as a directed acyclic graph (DAG), denoted by $G = (V, E)$, where V is the set of nodes and E the set of directed edges. A node s' is said to be a child of node s if and only if there exists a directed edge $(s \rightarrow s') \in E$; correspondingly, s is the parent of s' . The graph includes a unique root node $s_0 \in V$ with no incoming edges and a subset of terminal nodes $\mathcal{X} \subseteq V$ with no outgoing edges.

A positive reward function $R(x)$ is defined over the terminal nodes $x \in \mathcal{X}$. The objective of GFlowNets is to learn a stochastic forward policy $\mathcal{P}_F(s'|s)$ such that the probability of reaching a terminal node $x \in \mathcal{X}$ is proportional to its associated reward $R(x)$. This is accomplished by generating sequences of transitions, where at each step, the agent selects a child node of the current state. In this work, we focus on deterministic environment dynamics, where each action uniquely determines the next state by traversing the corresponding edge in the DAG, as is standard in most existing GFlowNet studies [1, 3–6, 9, 10].

For training GFlowNets, [1] introduced a parameterized flow function and proposed the Flow-Matching (FM) objective, whose global minimization ensures that the induced policy satisfies the desired proportionality condition. Recent work [24] establishes a formal equivalence between GFlowNet training and entropy-regularized RL under specific settings: a discount factor $\gamma = 1$, an entropy regularization coefficient $\lambda = 1$, and a modified reward function defined by a fixed backward policy $\mathcal{P}_B(s|s')$ that samples parent nodes in the DAG in reverse from a given child node:

$$\tilde{R}(s, s') = \begin{cases} \log \mathcal{P}_B(s|s'), & \text{if } s \notin \mathcal{X} \cup \{s_f\}, \\ \log R(s), & \text{if } s \in \mathcal{X}, \\ 0, & \text{if } s = s_f, \end{cases} \quad (1)$$

where s_f denotes an additional absorbing state. Consequently, learning the forward policy reduces to solving the following entropy-regularized policy optimization problem:

$$\mathcal{P}_F^* = \arg \max_{\pi} \left(\lambda \mathcal{H}(\pi) + \mathbb{E}_{\pi} \left[\sum_{t=0}^{\infty} \gamma^t \tilde{R}(s_t, s_{t+1}) \right] \right), \quad (2)$$

where $\mathcal{H}(\pi) = \mathbb{E}_{\pi} [-\log \pi(s'|s)]$ denotes the causal entropy of the policy. The expectation \mathbb{E}_{π} is taken with respect to trajectories generated by $s_0 \sim P_0$ and $s_{t+1} \sim \pi(\cdot|s_t)$, where P_0 is the initial state distribution that corresponds to a Dirac delta distribution in the GFlowNet setting.

In this paper, we address the problem of training a GFlowNet using an offline dataset $\mathcal{D} = \{\tau_i = (s_0, s_1, \dots, s_{T_i}, R(s_{T_i}))\}_{i=1}^M$, which consists of trajectories of constructed objects generated by an unknown behavior policy, along with their corresponding ground-truth rewards.

2.2 Maximum causal entropy IRL

Maximum causal entropy inverse reinforcement learning (IRL) [25, 26] seeks to recover a reward function $r(s, s')$ that both explains expert behavior under a policy π_E and promotes maximum entropy in the learned policy. This objective is formalized as the following minimax optimization problem:

$$\text{minimize}_r \left(\max_{\pi} \left[\lambda \mathcal{H}(\pi) + \mathbb{E}_{\pi} \left(\sum_{t=0}^{\infty} \gamma^t r(s_t, s_{t+1}) \right) \right] \right) - \mathbb{E}_{\pi_E} \left[\sum_{t=0}^{\infty} \gamma^t r(s_t, s_{t+1}) \right], \quad (3)$$

where $\mathcal{H}(\pi)$ denotes the causal entropy of the policy π , consistent with its definition in Equation 2. In our approach, we adapt this framework to infer an edge-level reward function $R_E : E \rightarrow \mathbb{R}$ that reflects the expert policy’s preferences for allocating flow across specific edges in the graph.

3 Method

In this section, we introduce **Trajectory-Distilled GFlowNet (TD-GFN)**, a proxy-free training framework that eliminates the need to query rewards outside the dataset, thereby avoiding reliance on proxy reward models. Unlike prior methods that constrain the policy to remain close to the dataset [21, 22], TD-GFN achieves a more effective exploration–exploitation trade-off by strategically allocating attention across the environment DAG.

The overall training pipeline is illustrated in Figure 2. First, TD-GFN learns an *edge reward function* from a rebalanced dataset using inverse reinforcement learning (IRL). This function captures the relative importance of each edge in the environment DAG, providing principled guidance for policy learning. Leveraging these edge-level rewards, TD-GFN then prunes the DAG to remove low-utility transitions and trains the policy via prioritized backward sampling over the resulting subgraph. This design enables strategic generalization to broad, unseen regions of the state space while maintaining alignment with high-reward behaviors. The following subsections detail each component.

A comprehensive summary of the full training procedure is presented in Algorithm 1 (Appendix A). Notably, the contributions of TD-GFN are orthogonal to the specific training strategies employed after trajectory sampling, as discussed in Appendix D.5.

3.1 Edge rewards extraction via IRL

Motivated by the insight that different edges in the environment DAG contribute *unequally* to effective policy learning, we aim to quantify this disparity to enable more targeted and generalizable training.

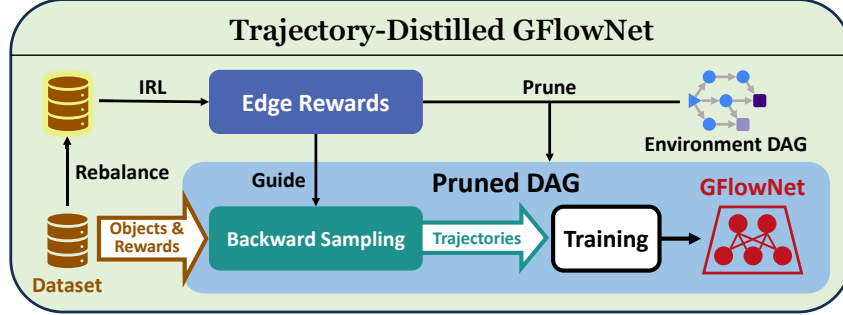


Figure 2: An overview of the complete training pipeline of the TD-GFN framework.

Nevertheless, measuring the contribution of individual transitions under the inherently stochastic nature of GFlowNet policies poses a fundamental challenge. To tackle this, we leverage the theoretical equivalence between GFlowNet training and entropy-regularized reinforcement learning (Equation 2) and applying the maximum causal entropy IRL framework [25, 26] (Equation 3) to extract a fine-grained *edge-level reward function* from offline trajectories. These learned edge rewards act as structured supervision signals that capture the relative importance of transitions, guiding the policy to generalize effectively across the environment DAG.

A central obstacle in applying IRL to offline data, however, lies in the fact that the behavior policy underlying the dataset may not reflect expert behavior. To mitigate this, we introduce a rebalancing strategy inspired by [27] that biases trajectory sampling according to the reward of terminal states. Specifically, when estimating expectations under the expert policy \mathbb{E}_{π_E} , we sample trajectories $\tau = (s_0, s_1, \dots, s_T) \in \mathcal{D}$ with probability $P(\tau) \propto R(s_T)$, thereby constructing a *rebalanced dataset* that more closely approximates the visitation distribution of an expert policy. This reweighting adjusts edge visitation frequencies to favor high-reward regions, enabling more meaningful reward inference.

Inspired by the well-known maximum causal entropy IRL framework GAIL [28], we adopt the following adversarial training objective based on the rebalanced dataset:

$$\begin{aligned} \text{minimize}_{\phi} \max_{\psi} \mathcal{L}(\psi, \phi) = \\ (\lambda \mathcal{H}(\pi_{\psi}) + \mathbb{E}_{s \sim \tilde{\mathcal{D}}, s' \sim \pi_{\psi}(\cdot|s)} [\log D_{\phi}(s, s')]) + \mathbb{E}_{(s, s') \sim \tilde{\mathcal{D}}} [\log (1 - D_{\phi}(s, s'))], \end{aligned} \quad (4)$$

where $\tilde{\mathcal{D}}$ denotes both the node and edge distributions (with slight abuse of notation), π_{ψ} is a parameterized policy and $D_{\phi} : E \rightarrow (0, 1)$ is a discriminative classifier, both optimized iteratively.

Nevertheless, the original GAIL framework induces a reward function that is strictly non-negative, making it inherently incapable of recovering the true underlying reward in our setting, which may include negative values (Equation 1). To address this limitation, we follow [29] and extract an unbiased edge-level reward function R_E from the classifier:

$$R_E(s, s') = \log D_{\phi}(s, s') - \log (1 - D_{\phi}(s, s')) \quad (5)$$

Intuitively, the learned edge reward reflects the degree to which an expert policy will prefer to traverse a given edge, thereby quantifying the edge’s importance for learning a high-quality GFlowNet policy. The complete edge reward extraction procedure is summarized in Algorithm 2 in Appendix A.

As shown in Figure 1(b) and Appendix D.2, the learned edge rewards exhibit strong generalization, assigning meaningful values even to transitions not observed in the dataset. This guides the policy to allocate attention across the entire environment DAG, rather than staying confined to regions near the training data, as in prior methods. Notably, such edge-level supervision aligns more closely with the original objective of GFlowNets: leveraging structured, multi-step decision-making to decompose the target distribution, rather than relying on proxy models for direct approximation. Next, we leverage these edge rewards to guide both DAG pruning and prioritized backward sampling of training trajectories, as illustrated in Figure 2.

3.2 Reward-guided pruning and prioritized backward sampling

Although the learned edge reward provides a meaningful signal at the transition level, directly incorporating it into the training objective introduces sensitivity to function approximation errors, which can distort the optimization process and degrade policy performance—mirroring the limitations commonly observed with proxy reward models. To enhance both the robustness and efficiency of the algorithm, we propose two indirect mechanisms for shaping the GFlowNet policy: *reward-guided pruning* and *prioritized backward sampling*.

Guided by the learned edge reward, TD-GFN strategically removes low-utility edges from the environment DAG $G = (V, E)$. Specifically, we approximate the distribution of edge rewards using a batch $\mathcal{D}_{R_E} = \{R_E(s_i, \text{selected}(\pi_\psi(\cdot | s_i)))\}_{i=1}^B$, where π_ψ denotes the imitation policy obtained during edge reward learning (Algorithm 2), serving as a surrogate for expert behavior. An edge $(s \rightarrow s')$ is pruned from the graph if it lies in the low-density region of the reward distribution:

$$R_E(s, s') < \text{mean}(\mathcal{D}_{R_E}) - K \cdot \text{std}(\mathcal{D}_{R_E}), \quad (6)$$

where K is a pruning threshold hyperparameter, and $\text{mean}(\cdot)$, $\text{std}(\cdot)$ denote the empirical mean and standard deviation over the sampled batch \mathcal{D}_{R_E} .

After applying this criterion, we remove all edges that are disconnected from the root node s_0 , resulting in a pruned subgraph $G' = (V', E')$ and an updated set of terminal nodes \mathcal{X}' . Notably, pruning is conducted over the full environment DAG, rather than being limited to dataset-observed transitions, enabling the retention of transitions that, while unobserved in the dataset, may potentially lead to high-reward regions.

This pruning approach concentrates learning on informative areas of the state space and improves training efficiency by reducing the complexity of model fitting [30, 31]. The resulting subgraph defines a more compact yet expressive action space that prioritizes structurally meaningful and high-reward trajectories, thereby supporting policy generalization beyond observed data while remaining anchored in reliable behavioral signals.

To train the policy more efficiently on the pruned graph, we additionally propose a prioritized backward sampling mechanism that selects training trajectories from high-value terminal nodes. Terminal states are sampled from the intersection of the pruned terminal set \mathcal{X}' and dataset-supported objects $\{s_{T_i}\}_{i=1}^M$, with probability proportional to their known rewards. From each sampled terminal node x , we recursively perform backward sampling toward the root s_0 using a learned backward policy \mathcal{P}_B , defined as:

$$\mathcal{P}_B(s_t | s_{t+1}) = \frac{\exp\{R_E(s_t, s_{t+1})\}}{\sum_{(s, s_{t+1}) \in E'} \exp\{R_E(s, s_{t+1})\}}, \quad (7)$$

This formulation is consistent with the reward shaping principles in Equation 1. By sharpening policy updates toward the most informative regions of the state space, this prioritized strategy reinforces the GFlowNet inductive bias of allocating sampling effort in proportion to reward, significantly improving sample efficiency [32, 33]. Moreover, when combined with the pruning method described above, it helps mitigate the under-exploitation of terminal nodes discussed in [34].

Finally, we optimize the policy on the pruned DAG using the Flow-Matching (FM) objective [1]. By setting $R(s) = 0$ for all non-terminal states s , the objective for each sampled trajectory τ is given by:

$$\mathcal{L}_{FM}(\tau; \theta) = \sum_{s' \in \tau} \left(\sum_{s: (s \rightarrow s') \in E'} F_\theta(s, s') - R(s') - \sum_{s'': (s' \rightarrow s'') \in E'} F_\theta(s', s'') \right)^2, \quad (8)$$

where $F_\theta(s, s')$ denotes the flow along edge $(s \rightarrow s')$. The resulting flow-based policy is then defined by sampling child states in proportion to the learned flows at each parent state.

4 Experiments

In this section, we empirically demonstrate the effectiveness of the proposed TD-GFN through extensive experiments. Specifically, we aim to answer the following questions: (i) Can TD-GFN effectively sample from the target reward distribution, and generate high-reward and diverse samples?

(ii) Is TD-GFN training efficient? (iii) Does TD-GFN consistently improve performance across different scenarios? We also conduct ablation studies to evaluate the individual contributions of each component within our method, as presented in Appendix D.4. Comprehensive task descriptions and implementation details of the algorithm are provided in Appendix C.

4.1 Hypergrid

We begin with experiments on the Hypergrid task [1], a D -dimensional grid environment with side length H , resulting in a discrete space of size H^D . High-reward modes are narrowly concentrated near the 2^D corners, making the task particularly challenging for both exploration-based and offline learning algorithms. Our main experiments are conducted on a 8^4 Hypergrid ($H = 8, D = 4$) following the setup in [1]. Additionally, in Appendix D.2, we visualize a 8×8 Hypergrid instance and illustrate the TD-GFN workflow on this task.

Due to the lack of existing proxy-free training methods for GFlowNets, we compare TD-GFN against a broad range of baselines trained on offline datasets. These include popular offline RL algorithms such as CQL [35] and IQL [36], imitation learning methods such as Behavior Cloning (BC) and GAIL [28], and the offline GFlowNet variant COFlowNet [22]. We additionally include a baseline termed *Dataset-GFN*, which trains a GFlowNet directly on offline trajectories without modification, serving as a vanilla proxy-free variant. For both offline RL and imitation learning methods, we adopt their soft RL formulations to enable stochastic policy sampling rather than pure reward maximization. To ensure a fair comparison, we train GAIL using the rebalanced dataset described in Section 3.1, which improves its performance relative to training on the original dataset. Accordingly, we evaluate GAIL using the imitation policy learned via Algorithm 2.

Each algorithm is evaluated using two standard metrics [1, 22, 37, 38]. The first is *Empirical L1 Error*, which measures the \mathcal{L}_1 distance between the empirical distribution $\pi(x)$ from model samples and the normalized reward distribution $p(x) = R(x)/Z$, computed as $\mathbb{E}[|\pi(x) - p(x)|]$. The second is *Modes Found*, defined as the number of distinct reward modes discovered during training.

As shown in Figure 3(a), when trained on an *Expert* dataset of 1,500 trajectories collected by a well-trained GFlowNet policy, all baseline methods require at least 30,000 state visits to uncover all 16 modes, whereas TD-GFN discovers all modes with fewer than 500 visits. Although both TD-GFN and COFlowNet achieve the lowest *Empirical L1 Error*, TD-GFN converges in less than half the number of state visits required by COFlowNet, demonstrating its superior training efficiency. Additional baseline analysis is provided in Appendix D.6.

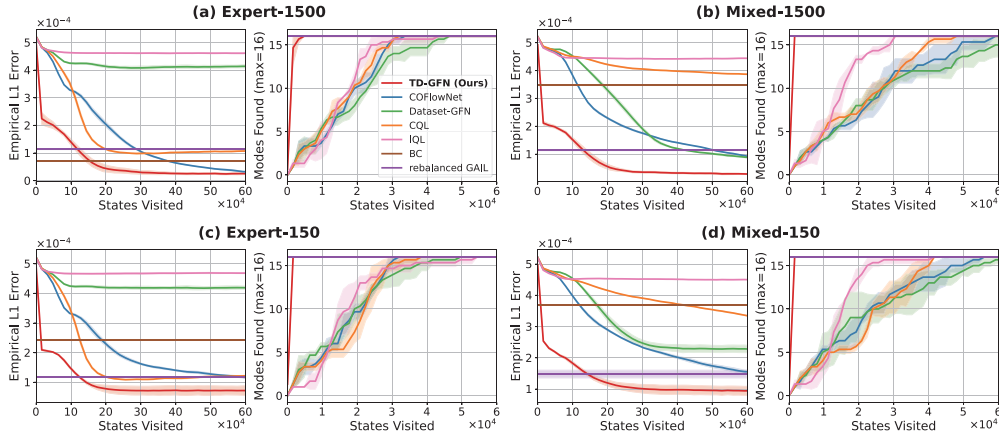


Figure 3: Performance comparison on the 8^4 Hypergrid task. The top row shows results using 1,500 trajectories from the *Expert* and *Mixed* datasets for policy training, while the bottom row shows results using only 150 trajectories. The solid line and shaded region represent the mean and standard deviation, respectively.

Robustness to Dataset Uncertainty We first assess the robustness of TD-GFN under dataset uncertainty by introducing greater variability in the training data. In the *Mixed* setting, we augment

the *Expert* dataset with an equal number of trajectories generated by a random policy similar to [27, 39], thereby introducing noise. In another setting, we significantly reduce the number of available trajectories—using only one-tenth of the original dataset—to simulate data scarcity as an additional source of uncertainty [40].

As shown in Figure 3, TD-GFN performs robustly under both types of uncertainty. It consistently models the target distribution more accurately and finds high-reward modes significantly faster than baseline methods. These results highlight TD-GFN’s resilience to noisy and limited data. Further evaluation under extreme data scarcity appears in Appendix D.1.

Robustness to Behavior Policy Quality We also examine the sensitivity of TD-GFN to the quality of the behavior policy used during data collection. To this end, we construct two offline datasets. The first, denoted *Median*, is collected using a suboptimal GFlowNet trained for only half the number of steps required for convergence. The second, denoted *Bad*, is generated by a GFlowNet trained with an inverted reward function $IR = R^{-0.1}$, while the dataset still contains the true rewards.

As shown in Figure 4, TD-GFN adapts effectively in both scenarios, achieving faster alignment with the target reward distribution and recovering all reward modes earlier than baseline methods. Notably, when the behavior policy diverges substantially from the expert (*Bad*), TD-GFN exhibits significantly more accurate distribution modeling, underscoring its robustness under adverse conditions.

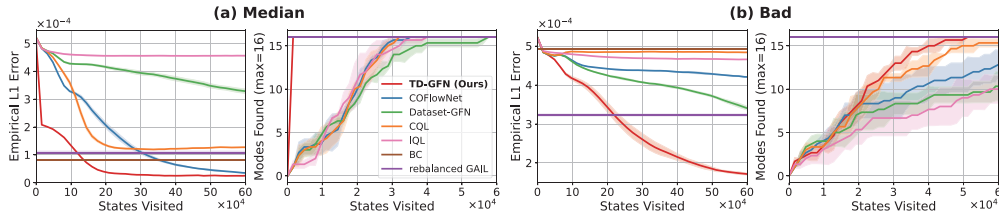


Figure 4: Performance comparison on the 8^4 Hypergrid task. Policies are trained using the *Median* and *Bad* datasets, each consisting of 1, 500 trajectories. The solid line and shaded region represent the mean and standard deviation, respectively.

4.2 Biosequence Design

We next evaluate the performance of TD-GFN on a more challenging task—designing anti-microbial peptides (AMPs), i.e., short protein sequences—introduced in [3]. The experimental setup leverages two datasets curated from the DBAASP database [41]: one for training a proxy model to approximate reward values, and another for training an oracle that provides ground-truth reward labels.

Following the methodology of [1], we train a Proxy-GFN using the proxy model and compare its performance with TD-GFN, as well as with other baseline methods previously evaluated on the Hypergrid task (Section 4.1). All methods are trained on the same dataset used for proxy learning, which includes 3, 219 positive AMPs and 4, 761 non-AMPs.

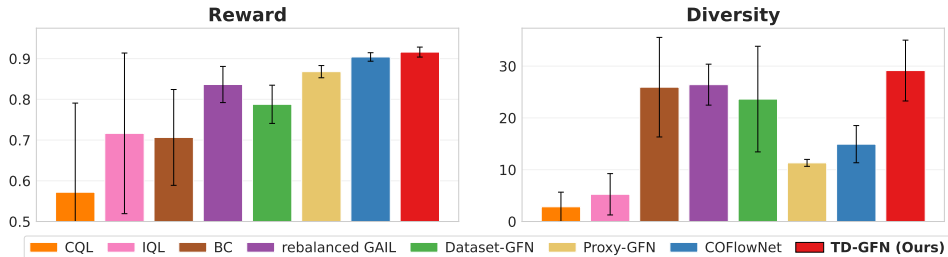


Figure 5: Comparison of reward and diversity among the top 100 sequences ranked by reward. The *Diversity* metric is defined in Appendix C.2. All results are averaged over three random seeds, and error bars indicate the standard deviation.

We generate 5,000 sequences using each learned policy and report the reward and diversity metrics for the top 100 sequences ranked by reward, as shown in Figure 5. TD-GFN consistently produces sequences with the highest rewards and greatest diversity. Notably, although rebalanced GAIL merely imitates the policy implied by the rebalanced dataset, it still achieves strong performance—outperforming Dataset-GFN, which is trained directly on the dataset trajectories, in both reward and diversity. These findings highlight the effectiveness of our dataset rebalancing strategy.

4.3 Molecule Design

We further evaluate the effectiveness of our method on a real-world molecular design task introduced by [1]. A training dataset is constructed to simulate historical data produced by human experts, which comprises 1,500 trajectories generated by a well-trained GFlowNet policy, with corresponding reward values provided by an oracle [1].

Table 1: Comparison of methods on the Molecule Design task. The *Convergence* column indicates the number of trajectories required for policy convergence. Results are reported as mean \pm standard deviation over three random seeds. Bold numbers indicate the best performance in each column.

Method	Reward-10 (\uparrow)	Reward-100 (\uparrow)	Reward-1000 (\uparrow)	Convergence (\downarrow)
CQL	7.069	6.643	5.401	0.803×10^4
IQL	6.902	5.980	4.628	4.104×10^4
BC	7.652 ± 0.053	7.223 ± 0.035	6.459 ± 0.016	/
GAIL	7.528 ± 0.068	7.152 ± 0.085	6.406 ± 0.033	/
Proxy-GFN	7.625 ± 0.063	7.281 ± 0.067	6.636 ± 0.097	43.735×10^4
Dataset-GFN	7.550 ± 0.045	7.198 ± 0.018	6.474 ± 0.018	6.030×10^4
FM-COFlowNet	7.582 ± 0.057	7.201 ± 0.015	6.485 ± 0.016	5.829×10^4
QM-COFlowNet	7.611 ± 0.020	7.296 ± 0.022	6.638 ± 0.010	4.423×10^4
TD-GFN (Ours)	7.733 ± 0.036	7.450 ± 0.037	6.810 ± 0.035	2.749×10^4

Following the approach used in the Biosequence Design task (Section 4.2), we train a proxy model on this dataset using the architecture and methodology commonly adopted in prior GFlowNet research [1, 9, 24, 42, 43], resulting in a baseline referred to as Proxy-GFN. Moreover, [22] proposed an enhanced COFlowNet incorporating quantile matching [38] to improve candidate diversity. Accordingly, we evaluate both the original and quantile-augmented variants (FM/QM).

We report the average top- k reward obtained from 5,000 samples generated by policies trained with different algorithms, along with the number of training trajectories required for policy convergence, in Table 1. Due to the instability of offline RL methods under sparse rewards, results for CQL and IQL are reported using only their best-performing random seed.

As shown in the table, CQL converges fastest in terms of sample efficiency but struggles to generate a diverse set of high-reward candidates, resulting in substantially lower top- k average rewards than GFN-based and even imitation learning methods. Excluding CQL, TD-GFN achieves the best performance in discovering high-reward molecules with the fewest trajectories, highlighting its training effectiveness and efficiency.

In contrast, although Proxy-GFN performs competitively and is comparable to QM-COFlowNet in terms of reward quality, it requires significantly more trajectory rollouts during training. This further underscores the efficiency of learning directly from offline data. Additional comparisons of training time and computational resource usage are provided in Appendix D.3.

To evaluate the diversity of molecules generated by TD-GFN, we measure the number of distinct high-reward modes identified by each algorithm. Modes are defined as clusters of high-reward molecules based on Tanimoto similarity [44]. As shown in Figure 6, TD-GFN consistently

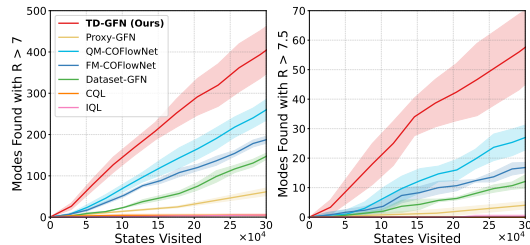


Figure 6: Number of high-reward modes (reward > 7 and > 7.5) discovered during training in the Molecule Design task. The solid line and shaded region represent the mean and standard deviation, respectively.

discovers 1.5 to 2 times more high-reward modes than the strongest baselines, indicating superior exploration. Notably, despite incorporating DAG pruning, TD-GFN does not overfit to narrow regions of the search space. Instead, it guides the policy toward a broader set of high-reward regions, balancing targeted exploitation with diverse exploration.

5 Conclusion

We introduced **Trajectory-Distilled GFlowNet (TD-GFN)**, a proxy-free training framework for learning GFlowNets from offline datasets without requiring out-of-distribution reward queries. Leveraging edge-level supervision learned via IRL, TD-GFN consistently guides the policy toward improved performance and training efficiency through DAG pruning and prioritized backward trajectory sampling. Extensive experiments validate the effectiveness of the proposed approach.

References

- [1] E. Bengio, M. Jain, M. Korablyov, D. Precup, and Y. Bengio, “Flow network based generative models for non-iterative diverse candidate generation,” *Advances in Neural Information Processing Systems*, vol. 34, pp. 27 381–27 394, 2021.
- [2] Y. Bengio, S. Lahlou, T. Deleu, E. J. Hu, M. Tiwari, and E. Bengio, “Gflownet foundations,” *Journal of Machine Learning Research*, vol. 24, no. 210, pp. 1–55, 2023.
- [3] M. Jain, E. Bengio, A. Hernandez-Garcia, J. Rector-Brooks, B. F. Dossou, C. A. Ekbote, J. Fu, T. Zhang, M. Kilgour, D. Zhang *et al.*, “Biological sequence design with gflownets,” in *International Conference on Machine Learning*. PMLR, 2022, pp. 9786–9801.
- [4] N. Zhang, J. Yang, Z. Cao, and X. Chi, “Adversarial generative flow network for solving vehicle routing problems,” in *The Thirteenth International Conference on Learning Representations*, 2025. [Online]. Available: <https://openreview.net/forum?id=tBom4xOW1H>
- [5] E. J. Hu, M. Jain, E. Elmoznino, Y. Kaddar, G. Lajoie, Y. Bengio, and N. Malkin, “Amortizing intractable inference in large language models,” in *The Twelfth International Conference on Learning Representations*, 2024. [Online]. Available: <https://openreview.net/forum?id=Ouj6p4ca60>
- [6] Z. Liu, T. Z. Xiao, W. Liu, Y. Bengio, and D. Zhang, “Efficient diversity-preserving diffusion alignment via gradient-informed GFlownets,” in *The Thirteenth International Conference on Learning Representations*, 2025. [Online]. Available: <https://openreview.net/forum?id=Aye5wL6TCn>
- [7] T. da Silva, E. Silva, A. Góis, D. Heider, S. Kaski, D. Mesquita, and A. Ribeiro, “Human-in-the-loop causal discovery under latent confounding using ancestral gflownets,” *arXiv preprint arXiv:2309.12032*, 2023.
- [8] C. Angermueller, D. Dohan, D. Belanger, R. Deshpande, K. Murphy, and L. Colwell, “Model-based reinforcement learning for biological sequence design,” in *International Conference on Learning Representations*, 2020. [Online]. Available: <https://openreview.net/forum?id=HklxbgBKvr>
- [9] H. Jang, M. Kim, and S. Ahn, “Learning energy decompositions for partial inference of gflownets,” *arXiv preprint arXiv:2310.03301*, 2023.
- [10] M. Kim, T. Yun, E. Bengio, D. Zhang, Y. Bengio, S. Ahn, and J. Park, “Local search gflownets,” *URL <https://arxiv.org/abs/2310>*, vol. 2710, 2024.
- [11] Z. JIANG, X. Feng, P. Weng, Y. Zhu, Y. Song, T. Zhou, Y. Hu, T. Lv, and C. Fan, “Reinforcement learning from imperfect corrective actions and proxy rewards,” in *The Thirteenth International Conference on Learning Representations*, 2025. [Online]. Available: <https://openreview.net/forum?id=JTji0Jfh5a>
- [12] S. Wang, S. Zhang, J. Zhang, R. Hu, X. Li, T. Zhang, J. Li, F. Wu, G. Wang, and E. Hovy, “Reinforcement learning enhanced llms: A survey,” *arXiv preprint arXiv:2412.10400*, 2024.

- [13] C. Laidlaw, S. Singhal, and A. Dragan, “Correlated proxies: A new definition and improved mitigation for reward hacking,” in *The Thirteenth International Conference on Learning Representations*, 2025. [Online]. Available: <https://openreview.net/forum?id=msEr27EejF>
- [14] D. M. Ziegler, N. Stiennon, J. Wu, T. B. Brown, A. Radford, D. Amodei, P. Christiano, and G. Irving, “Fine-tuning language models from human preferences,” *arXiv preprint arXiv:1909.08593*, 2019.
- [15] D. Dalrymple, J. Skalse, Y. Bengio, S. Russell, M. Tegmark, S. Seshia, S. Omohundro, C. Szegedy, B. Goldhaber, N. Ammann *et al.*, “Towards guaranteed safe ai: A framework for ensuring robust and reliable ai systems,” *arXiv preprint arXiv:2405.06624*, 2024.
- [16] X. Chen, S. Wang, J. McAuley, D. Jannach, and L. Yao, “On the opportunities and challenges of offline reinforcement learning for recommender systems,” *ACM Transactions on Information Systems*, vol. 42, no. 6, pp. 1–26, 2024.
- [17] Y. Xie, X. Guo, C. Wang, K. Liu, and L. Chen, “Advdiffuser: Generating adversarial safety-critical driving scenarios via guided diffusion,” in *2024 IEEE/RSJ International Conference on Intelligent Robots and Systems (IROS)*. IEEE, 2024, pp. 9983–9989.
- [18] M. Jain, T. Deleu, J. Hartford, C.-H. Liu, A. Hernandez-Garcia, and Y. Bengio, “Gflownets for ai-driven scientific discovery,” *Digital Discovery*, vol. 2, no. 3, pp. 557–577, 2023.
- [19] A. H. Cheng, C. T. Ser, M. Skreta, A. Guzmán-Cordero, L. Thiede, A. Burger, A. Aldossary, S. X. Leong, S. Pablo-García, F. Strieth-Kalthoff *et al.*, “Spiers memorial lecture: How to do impactful research in artificial intelligence for chemistry and materials science,” *Faraday Discussions*, vol. 256, pp. 10–60, 2025.
- [20] L. Ouyang, J. Wu, X. Jiang, D. Almeida, C. Wainwright, P. Mishkin, C. Zhang, S. Agarwal, K. Slama, A. Ray *et al.*, “Training language models to follow instructions with human feedback,” *Advances in neural information processing systems*, vol. 35, pp. 27 730–27 744, 2022.
- [21] H. Wang, Y. Li, yunfeng shao, and J. HAO, “Regularized offline GFlowNets,” 2023. [Online]. Available: <https://openreview.net/forum?id=kbhUUAMZmQT>
- [22] Y. Zhang, X. Yu, X. Wang, Z. Sun, C. Zhang, P. Wang, and Y. Wang, “COFlowNet: Conservative constraints on flows enable high-quality candidate generation,” in *The Thirteenth International Conference on Learning Representations*, 2025. [Online]. Available: <https://openreview.net/forum?id=tXUKT709OJ>
- [23] L. Atanackovic and E. Bengio, “Investigating generalization behaviours of generative flow networks,” *arXiv preprint arXiv:2402.05309*, 2024.
- [24] D. Tiapkin, N. Morozov, A. Naumov, and D. P. Vetrov, “Generative flow networks as entropy-regularized rl,” in *International Conference on Artificial Intelligence and Statistics*. PMLR, 2024, pp. 4213–4221.
- [25] B. D. Ziebart, A. L. Maas, J. A. Bagnell, A. K. Dey *et al.*, “Maximum entropy inverse reinforcement learning,” in *Aaai*, vol. 8. Chicago, IL, USA, 2008, pp. 1433–1438.
- [26] B. D. Ziebart, J. A. Bagnell, and A. K. Dey, “Modeling interaction via the principle of maximum causal entropy,” in *Proceedings of the 27th International Conference on International Conference on Machine Learning*, ser. ICML’10. Madison, WI, USA: Omnipress, 2010, p. 1255–1262.
- [27] Z.-W. Hong, P. Agrawal, R. T. d. Combes, and R. Laroche, “Harnessing mixed offline reinforcement learning datasets via trajectory weighting,” *arXiv preprint arXiv:2306.13085*, 2023.
- [28] J. Ho and S. Ermon, “Generative adversarial imitation learning,” *Advances in neural information processing systems*, vol. 29, 2016.
- [29] I. Kostrikov, K. K. Agrawal, D. Dwibedi, S. Levine, and J. Tompson, “Discriminator-actor-critic: Addressing sample inefficiency and reward bias in adversarial imitation learning,” *arXiv preprint arXiv:1809.02925*, 2018.

- [30] T. Zahavy, M. Haroush, N. Merlis, D. J. Mankowitz, and S. Mannor, “Learn what not to learn: Action elimination with deep reinforcement learning,” *Advances in neural information processing systems*, vol. 31, 2018.
- [31] Y. Zhang, P. Abbeel, and L. Pinto, “Automatic curriculum learning through value disagreement,” *Advances in Neural Information Processing Systems*, vol. 33, pp. 7648–7659, 2020.
- [32] M. W. Shen, E. Bengio, E. Hajiramezanali, A. Loukas, K. Cho, and T. Biancalani, “Towards understanding and improving gflownet training,” in *International conference on machine learning*. PMLR, 2023, pp. 30 956–30 975.
- [33] T. Schaul, J. Quan, I. Antonoglou, and D. Silver, “Prioritized experience replay,” *arXiv preprint arXiv:1511.05952*, 2015.
- [34] H. Jang, Y. Jang, M. Kim, J. Park, and S. Ahn, “Pessimistic backward policy for gflownets,” *arXiv preprint arXiv:2405.16012*, 2024.
- [35] A. Kumar, A. Zhou, G. Tucker, and S. Levine, “Conservative q-learning for offline reinforcement learning,” *Advances in neural information processing systems*, vol. 33, pp. 1179–1191, 2020.
- [36] I. Kostrikov, A. Nair, and S. Levine, “Offline reinforcement learning with implicit q-learning,” *arXiv preprint arXiv:2110.06169*, 2021.
- [37] L. Pan, D. Zhang, A. Courville, L. Huang, and Y. Bengio, “Generative augmented flow networks,” *arXiv preprint arXiv:2210.03308*, 2022.
- [38] D. Zhang, L. Pan, R. T. Chen, A. Courville, and Y. Bengio, “Distributional gflownets with quantile flows,” *arXiv preprint arXiv:2302.05793*, 2023.
- [39] C. Cao, Z. Yan, R. Lu, J. Tan, and X. Wang, “Offline goal-conditioned reinforcement learning for safety-critical tasks with recovery policy,” in *2024 IEEE International Conference on Robotics and Automation (ICRA)*. IEEE, 2024, pp. 2838–2844.
- [40] S. Depeweg, J.-M. Hernandez-Lobato, F. Doshi-Velez, and S. Udfluft, “Decomposition of uncertainty in bayesian deep learning for efficient and risk-sensitive learning,” in *International conference on machine learning*. PMLR, 2018, pp. 1184–1193.
- [41] M. Pirtskhalava, A. A. Armstrong, M. Grigolava, M. Chubinidze, E. Alimbarashvili, B. Vishnepolsky, A. Gabrielian, A. Rosenthal, D. E. Hurt, and M. Tartakovsky, “Dbaasp v3: database of antimicrobial/cytotoxic activity and structure of peptides as a resource for development of new therapeutics,” *Nucleic acids research*, vol. 49, no. D1, pp. D288–D297, 2021.
- [42] N. Malkin, M. Jain, E. Bengio, C. Sun, and Y. Bengio, “Trajectory balance: Improved credit assignment in gflownets,” *Advances in Neural Information Processing Systems*, vol. 35, pp. 5955–5967, 2022.
- [43] H. He, E. Bengio, Q. Cai, and L. Pan, “Random policy evaluation uncovers policies of generative flow networks,” 2025. [Online]. Available: <https://arxiv.org/abs/2406.02213>
- [44] D. Bajusz, A. Rácz, and K. Héberger, “Why is tanimoto index an appropriate choice for fingerprint-based similarity calculations?” *Journal of cheminformatics*, vol. 7, pp. 1–13, 2015.
- [45] S. Mohammadpour, E. Bengio, E. Frejinger, and P.-L. Bacon, “Maximum entropy gflownets with soft q-learning,” in *International Conference on Artificial Intelligence and Statistics*. PMLR, 2024, pp. 2593–2601.
- [46] N. Malkin, S. Lahlou, T. Deleu, X. Ji, E. Hu, K. Everett, D. Zhang, and Y. Bengio, “Gflownets and variational inference,” *URL <https://arxiv.org/abs/2210.00580>*, 2023.
- [47] H. Zimmermann, F. Lindsten, J.-W. van de Meent, and C. A. Naesseth, “A variational perspective on generative flow networks,” *Transactions on Machine Learning Research*, 2023. [Online]. Available: <https://openreview.net/forum?id=AZ4GobeSLq>

- [48] K. Madan, J. Rector-Brooks, M. Korablyov, E. Bengio, M. Jain, A. C. Nica, T. Bosc, Y. Bengio, and N. Malkin, “Learning gflownets from partial episodes for improved convergence and stability,” in *International Conference on Machine Learning*. PMLR, 2023, pp. 23 467–23 483.
- [49] L. Pan, N. Malkin, D. Zhang, and Y. Bengio, “Better training of gflownets with local credit and incomplete trajectories,” in *International Conference on Machine Learning*. PMLR, 2023, pp. 26 878–26 890.
- [50] T. Gritsaev, N. Morozov, S. Samsonov, and D. Tiapkin, “Optimizing backward policies in gflownets via trajectory likelihood maximization,” *arXiv preprint arXiv:2410.15474*, 2024.
- [51] M. Kim, S. Choi, T. Yun, E. Bengio, L. Feng, J. Rector-Brooks, S. Ahn, J. Park, N. Malkin, and Y. Bengio, “Adaptive teachers for amortized samplers,” *arXiv preprint arXiv:2410.01432*, 2024.
- [52] E. Lau, S. Lu, L. Pan, D. Precup, and E. Bengio, “Qgfn: Controllable greediness with action values,” *Advances in neural information processing systems*, vol. 37, pp. 81 645–81 676, 2024.
- [53] K. Madan, A. Lamb, E. Bengio, G. Berseth, and Y. Bengio, “Towards improving exploration through sibling augmented gflownets,” in *The Thirteenth International Conference on Learning Representations*, 2025.
- [54] T. Silva, E. de Souza da Silva, and D. Mesquita, “On divergence measures for training GFlowNets,” in *The Thirty-eighth Annual Conference on Neural Information Processing Systems*, 2024. [Online]. Available: <https://openreview.net/forum?id=N5H4z0Pzvn>
- [55] R. Hu, Y. Zhang, Z. Li, and L. Huang, “Beyond squared error: Exploring loss design for enhanced training of generative flow networks,” *arXiv preprint arXiv:2410.02596*, 2024.
- [56] L. Pan, D. Zhang, M. Jain, L. Huang, and Y. Bengio, “Stochastic generative flow networks,” in *Uncertainty in Artificial Intelligence*. PMLR, 2023, pp. 1628–1638.
- [57] S. Lahlou, T. Deleu, P. Lemos, D. Zhang, A. Volokhova, A. Hernández-García, L. N. Ezzine, Y. Bengio, and N. Malkin, “A theory of continuous generative flow networks,” in *International Conference on Machine Learning*. PMLR, 2023, pp. 18 269–18 300.
- [58] L. Brunswic, Y. Li, Y. Xu, Y. Feng, S. Jui, and L. Ma, “A theory of non-acyclic generative flow networks,” in *Proceedings of the AAAI Conference on Artificial Intelligence*, vol. 38, no. 10, 2024, pp. 11 124–11 131.
- [59] Y. Chen and L. Mauch, “Order-preserving GFlowNets,” in *The Twelfth International Conference on Learning Representations*, 2024. [Online]. Available: <https://openreview.net/forum?id=VXDPXuq4oG>
- [60] M. Jain, S. C. Rappaport, A. Hernández-García, J. Rector-Brooks, Y. Bengio, S. Miret, and E. Bengio, “Multi-objective gflownets,” in *International conference on machine learning*. PMLR, 2023, pp. 14 631–14 653.
- [61] Y. Zhu, J. Wu, C. Hu, J. Yan, T. Hou, J. Wu *et al.*, “Sample-efficient multi-objective molecular optimization with gflownets,” *Advances in Neural Information Processing Systems*, vol. 36, pp. 79 667–79 684, 2023.
- [62] J. Roy, P.-L. Bacon, C. Pal, and E. Bengio, “Goal-conditioned gflownets for controllable multi-objective molecular design,” *arXiv preprint arXiv:2306.04620*, 2023.
- [63] P. M. Ghari, A. Tseng, G. Eraslan, R. Lopez, T. Biancalani, G. Scalia, and E. Hajiramezanali, “Generative flow networks assisted biological sequence editing,” in *NeurIPS 2023 Generative AI and Biology (GenBio) Workshop*, 2023.
- [64] D. Zhang, H. Dai, N. Malkin, A. Courville, Y. Bengio, and L. Pan, “Let the flows tell: Solving graph combinatorial problems with GFlowNets,” in *Thirty-seventh Conference on Neural Information Processing Systems*, 2023. [Online]. Available: <https://openreview.net/forum?id=sTjW3JHs2V>

- [65] M. Kim, S. Choi, J. Son, H. Kim, J. Park, and Y. Bengio, “Ant colony sampling with gflownets for combinatorial optimization,” *CoRR*, vol. abs/2403.07041, 2024. [Online]. Available: <https://doi.org/10.48550/arXiv.2403.07041>
- [66] D. Zhang, N. Malkin, Z. Liu, A. Volokhova, A. Courville, and Y. Bengio, “Generative flow networks for discrete probabilistic modeling,” in *International Conference on Machine Learning*. PMLR, 2022, pp. 26 412–26 428.
- [67] T. Deleu, A. Góis, C. Emezue, M. Rankawat, S. Lacoste-Julien, S. Bauer, and Y. Bengio, “Bayesian structure learning with generative flow networks,” in *Uncertainty in Artificial Intelligence*. PMLR, 2022, pp. 518–528.
- [68] S. Liu, Q. Cai, Z. He, B. Sun, J. McAuley, D. Zheng, P. Jiang, and K. Gai, “Generative flow network for listwise recommendation,” in *Proceedings of the 29th ACM SIGKDD Conference on Knowledge Discovery and Data Mining*, 2023, pp. 1524–1534.
- [69] F. Yu, L. Jiang, H. Kang, S. Hao, and L. Qin, “Flow of reasoning: Training llms for divergent problem solving with minimal examples,” *arXiv preprint arXiv:2406.05673*, 2024.
- [70] S. Venkatraman, M. Jain, L. Scimeca, M. Kim, M. Sendera, M. Hasan, L. Rowe, S. Mittal, P. Lemos, E. Bengio, A. Adam, J. Rector-Brooks, Y. Bengio, G. Berseth, and N. Malkin, “Amortizing intractable inference in diffusion models for vision, language, and control,” in *The Thirty-eighth Annual Conference on Neural Information Processing Systems*, 2024. [Online]. Available: <https://openreview.net/forum?id=gVTkMsaaGI>
- [71] A. Y. Ng, S. Russell *et al.*, “Algorithms for inverse reinforcement learning.” in *Icml*, vol. 1, no. 2, 2000, p. 2.
- [72] J. Fu, K. Luo, and S. Levine, “Learning robust rewards with adversarial inverse reinforcement learning,” *arXiv preprint arXiv:1710.11248*, 2017.
- [73] I. Kostrikov, O. Nachum, and J. Tompson, “Imitation learning via off-policy distribution matching,” *arXiv preprint arXiv:1912.05032*, 2019.
- [74] D. Garg, S. Chakraborty, C. Cundy, J. Song, and S. Ermon, “Iq-learn: Inverse soft-q learning for imitation,” *Advances in Neural Information Processing Systems*, vol. 34, pp. 4028–4039, 2021.
- [75] F.-M. Luo, X. Cao, R.-J. Qin, and Y. Yu, “Transferable reward learning by dynamics-agnostic discriminator ensemble,” *arXiv preprint arXiv:2206.00238*, 2022.
- [76] F.-M. Luo, T. Xu, X. Cao, and Y. Yu, “Reward-consistent dynamics models are strongly generalizable for offline reinforcement learning,” *arXiv preprint arXiv:2310.05422*, 2023.
- [77] W. Jin, R. Barzilay, and T. Jaakkola, “Junction tree variational autoencoder for molecular graph generation,” in *International conference on machine learning*. PMLR, 2018, pp. 2323–2332.
- [78] J. Gilmer, S. S. Schoenholz, P. F. Riley, O. Vinyals, and G. E. Dahl, “Neural message passing for quantum chemistry,” in *International conference on machine learning*. PMLR, 2017, pp. 1263–1272.

Supplementary Materials

A	Algorithm Pseudocode	16
B	Related works	17
C	Experimental details	17
C.1	Hypergrid	17
C.2	Biosequence Design	18
C.3	Molecule Design	18
C.4	Policy Model Architectures and Hyperparameters	18
D	Additional experimental results	19
D.1	Algorithm trained on extremely limited data	19
D.2	Algorithm Visualization on Hypergrid	20
D.3	Time consumption and resource usage	20
D.4	Ablation Study	21
D.5	Orthogonality to Training Paradigms	22
D.6	Discussion on Baseline Performance	23
E	Future Directions	24

A Algorithm Pseudocode

Algorithm 1 Trajectory-Distilled GFlowNet (TD-GFN)

- 1: **Input:** Offline dataset $\mathcal{D} = \{\tau_i = (s_0, \dots, s_{T_i}, R(s_{T_i}))\}_{i=1}^M$; number of training iterations N ; batch size B ; GFlowNet learning rate η .
- 2: **Phase 1: Edge Reward Extraction**
- 3: Learn edge rewards $R_E(s, s')$ and the imitation policy π_ψ via Algorithm 2.
- 4: **Phase 2: DAG Pruning**
- 5: Collect edge rewards \mathcal{D}_{R_E} using $R_E(s, s')$ and π_ψ .
- 6: Prune the environment DAG $G = (V, E)$ based on the thresholding rule defined in Equation 6.
- 7: Remove disconnected edges to obtain the pruned DAG $G' = (V', E')$.
- 8: **Phase 3: Policy Training**
- 9: Initialize the GFlowNet flow function F_θ .
- 10: **for** $n = 1$ to N **do**
- 11: Initialize a batch of trajectories $\mathcal{T} = \emptyset$.
- 12: **for** $j = 1$ to B **do**
- 13: Sample a terminal node $x_j \in \mathcal{X}' \cap \{s_{T_i}\}_{i=1}^M$ with probability $P(x) \propto R(x)$.
- 14: Initialize a trajectory $\tau_j = \emptyset, s_{now} = x_j, s_{pre} = x_j$.
- 15: **while** $s_{now} \neq s_0$ **do**
- 16: Sample $s_{pre} \sim \mathcal{P}_B(\cdot | s_{now})$, where \mathcal{P}_B is defined in Equation 7 over G' .
- 17: $\tau_j = \tau_j \cup \{(s_{pre} \rightarrow s_{now})\}$.
- 18: $s_{now} = s_{pre}$
- 19: **end while** // Backward sampling.
- 20: $\mathcal{T} = \mathcal{T} \cup \{\tau_j\}$.
- 21: **end for** // Backward sample trajectories.
- 22: Optimize F_θ with \mathcal{T} using the FM loss over G' , as formulated in Equation 8. // Update flow function
- 23: **end for**
- 24: Extract the GFlowNet policy:

$$\mathcal{P}_F(s' | s) = \pi_\theta(s' | s) = \begin{cases} \frac{F_\theta(s, s')}{\sum_{(s \rightarrow s'') \in E'} F_\theta(s, s'')}, & \text{if } (s \rightarrow s') \in E', \\ 0, & \text{otherwise.} \end{cases}$$

- // Obtain policy from flow
- 25: **Output:** Trained GFlowNet policy \mathcal{P}_F .
-

Algorithm 2 Edge Reward Extraction

- 1: **Input:** Offline dataset $\mathcal{D} = \{\tau_i = (s_0, \dots, s_{T_i}, R(s_{T_i}))\}_{i=1}^M$; number of training iterations N' ; batch size B' ; policy learning rate α ; discriminator learning rate β .
 - 2: Initialize policy π_ψ and discriminator $D_\phi : E \rightarrow (0, 1)$ with random parameters ψ and ϕ .
 - 3: **for** $n = 1$ to N' **do**
 - 4: Initialize a batch of trajectories $\mathcal{T}' = \emptyset$.
 - 5: **for** $j = 1$ to B' **do**
 - 6: Sample a trajectory $\tau_j \in \mathcal{D}$ with probability $P(\tau_j) \propto R(s_{T_j})$.
 - 7: $\mathcal{T}' = \mathcal{T}' \cup \{\tau_j\}$.
 - 8: **end for** // Sample from the rebalanced dataset
 - 9: Extract edge transitions $\{(s, s')\}$ from \mathcal{T}' as a minibatch \bar{E} .
 - 10: Compute $\nabla_\phi L$ on \bar{E} ; update $\phi \leftarrow \phi - \beta \nabla_\phi L$. // Update discriminator
 - 11: Compute $\nabla_\psi L$ on \bar{E} ; update $\psi \leftarrow \psi - \alpha \nabla_\psi L$ or apply a policy gradient method. // Update policy
 - 12: **end for**
 - 13: Extract the edge reward function R_E according to Equation 5.
 - 14: **Output:** Edge reward function R_E ; imitation policy π_ψ .
-

B Related works

Generative Flow Networks (GFlowNets). GFlowNets [1, 2] are a class of generative models designed to sample compositional objects from an unnormalized reward distribution via sequential action selection. They have been theoretically linked to entropy-regularized reinforcement learning [24, 45] and variational inference [46, 47], offering a principled framework for distribution matching. Recent research has focused on improving GFlowNet training by proposing new balance conditions [42, 48], enhancing credit assignment through intermediate rewards [37, 49, 9], designing backward policies for improved sampling [34, 45, 32, 50], refining sampling and resampling strategies [23, 10, 51–53], and exploring alternative training objectives [54, 55]. Extensions to the GFlowNet framework have expanded its applicability to stochastic dynamics [56], continuous action spaces [57], non-acyclic transitions [58], and implicit reward feedback [59]. These advances have broadened the scope of GFlowNets, enabling impactful applications in molecule design [18, 60–62], biological sequence generation [3, 63], combinatorial optimization [4, 64, 65], causal inference [66, 67], recommendation systems [68], and fine-tuning of large language models [5, 69] and diffusion models [6, 70].

Inverse Reinforcement Learning (IRL). Inverse reinforcement learning (IRL) aims to recover a reward function that explains observed expert behavior in a Markov decision process [71]. Among its variants, maximum causal entropy IRL is particularly noteworthy, as it addresses reward ambiguity by formulating the objective as finding a policy that maximizes entropy while matching the observed expert behavior [25, 26]. Building on this framework, Generative Adversarial Imitation Learning (GAIL) [28] reinterprets imitation as a distribution matching problem via adversarial training, where a discriminator distinguishes expert from policy-generated trajectories, and its output serves as a learned reward for policy training. GAIL eliminates the need to explicitly solve the inner IRL loop, significantly improving scalability, and has inspired a broad class of Adversarial Imitation Learning (AIL) methods [72, 29, 73, 74]. This line of work has since been extended in various directions, including efforts to improve reward generalization and robustness [75, 76].

C Experimental details

C.1 Hypergrid

The Hypergrid task is a synthetic benchmark introduced in [1] to evaluate the exploration and generalization capabilities of GFlowNet algorithms. It presents a significant challenge due to its high-dimensional, sparse reward landscape.

The environment consists of a D -dimensional hypercubic grid with side length H , defining a discrete state space of size H^D . Each state corresponds to a coordinate $x = (x_1, \dots, x_D) \in \{0, \dots, H-1\}^D$. The agent starts at the origin $x = (0, \dots, 0)$ and can increment any individual coordinate by one at each step. A trajectory terminates when a special stop action is taken, and the reward is assigned based on the final state.

The reward function is designed to produce multiple sharp reward modes near the corners of the hypercube. Formally, the reward at a terminal state x is defined as:

$$R(x) = R_0 + R_1 \prod_{d=1}^D \mathbb{I}\left(\left|\frac{x_d}{H} - 0.5\right| > 0.25\right) + R_2 \prod_{d=1}^D \mathbb{I}\left(0.3 < \left|\frac{x_d}{H} - 0.5\right| < 0.4\right),$$

where $R_0 < R_1 \ll R_2$, and $\mathbb{I}(\cdot)$ denotes the indicator function. The first term, weighted by R_1 , introduces 2^D high-reward modes near the grid’s corners, while the second term, weighted by R_2 , creates even sparser regions of extremely high reward, thereby increasing the difficulty of discovering them through exploration alone.

Following the most challenging configuration proposed in [1], we set the environment parameters to $R_0 = 10^{-3}$, $R_1 = 0.5$, $R_2 = 2$. This configuration results in a highly multi-modal and sparsely rewarded environment, making it well-suited for evaluating the effectiveness of offline training strategies.

C.2 Biosequence Design

The Anti-Microbial Peptide (AMP) Design task, introduced in [3], is a realistic sequence generation benchmark aimed at designing short peptide sequences with strong anti-microbial properties.

The agent constructs sequences by selecting amino acids from a fixed vocabulary of 20 standard residues, with a maximum sequence length of 50. At each time step, the agent chooses either an amino acid or a special end-of-sequence token, proceeding in a left-to-right manner. As a result, the transition structure forms a tree.

Notably, when the environment DAG degenerates into a tree, the prioritized backward sampling strategy in TD-GFN simplifies to sampling trajectories from the dataset in proportion to their terminal rewards. Despite this simplification, TD-GFN remains effective on this task, which presents substantial challenges due to the large combinatorial space of valid sequences ($\approx 20^{50}$) and the extreme sparsity of high-reward regions.

In our experiments, we adopt the *Diversity* metric to evaluate algorithmic performance, following the methodology in [3]. For a set of biological sequences C , the metric is defined as:

$$\text{Diversity}(C) = \frac{\sum_{x_i, x_j \in C} \text{Lev}(x_i, x_j)}{|C|(|C| - 1)},$$

where $\text{Lev}(\cdot, \cdot)$ denotes the Levenshtein distance. All environmental parameters are kept consistent with those used in [3].

C.3 Molecule Design

We evaluate our method on a fragment-based molecular generation task targeting protein binding affinity, specifically for soluble epoxide hydrolase (sEH). The goal is to construct candidate molecules with high predicted affinity for the target protein. Molecules are generated sequentially using the junction tree framework introduced in [77], where each action involves selecting an attachment atom and adding a fragment from a predefined vocabulary of 105 building blocks.

The reward is defined as the negative binding energy between the generated molecule and the target protein, as predicted by an oracle model pre-trained on 300k molecules, following the setup in [1]. To balance reward maximization with output diversity, the final reward is modulated using a reward exponent ω , such that $R'(x) = R(x)^\omega$, where $R(x)$ denotes the raw oracle prediction. All environmental parameters, including ω , are kept consistent with those used in [1].

C.4 Policy Model Architectures and Hyperparameters

Across the experimental tasks presented in this work, we adopt the model architectures listed in Table 2 as the backbone structures for the policy networks.

Table 2: Policy network architectures used across different experimental tasks.

Task	Model architecture
Hypergrid	MLP([input, 256, 256, output])
Biosequence Design	MLP([input, 128, 128, output])
Molecule Design	MPNN [78] v4

Key algorithmic hyperparameters used across different tasks and methods are summarized in Table 3. These values were selected through empirical tuning to ensure stable training and fair comparisons among baselines.³ Specifically, the pruning threshold coefficient K is tuned by selecting the value that yields the highest ratio of retained expert transitions to retained randomly selected transitions.

³Our implementation of COFlowNet is based on the official open-source repository available at <https://github.com/yuxuan9982/COFlowNet>.

Table 3: Hyperparameters used across different tasks and methods.

Method	Hyperparameter	Task	Value
All	Policy learning rate η	Hypergrid	1×10^{-5}
		Molecule Design	1×10^{-4}
		Biosequence Design	1×10^{-3}
	Entropy coef. λ Seeds	All	0.01
		All	0,1,2
TD-GFN	Pruning coef. K	Hypergrid	7.0
		Molecule Design	1.0
		Biosequence Design	2.0
	Actor learning rate α	Hypergrid	1×10^{-5}
		Molecule Design	1×10^{-4}
		Biosequence Design	1×10^{-3}
	Discriminator learning rate β	Hypergrid	3×10^{-5}
Biosequence Design		3×10^{-3}	
COFlowNet	Regularizing coef. 1	Hypergrid	1.0
		Molecule Design	1.0
		Biosequence Design	/
	Regularizing coef. 2	Hypergrid	1.0
		Biosequence Design	25.0
IQL	Expectile	Hypergrid	0.9
		Molecule Design	0.9
		Biosequence Design	0.8
BC	Loss	All	Cross Entropy Loss

D Additional experimental results

D.1 Algorithm trained on extremely limited data

To further assess the robustness of TD-GFN under extreme data scarcity, we conduct experiments on the $H = 8$, $D = 4$ Hypergrid environment using only 30 training trajectories, as illustrated in Figure 7. In this setting, algorithms are prone to overfitting due to the limited data. For example, both COFlowNet and CQL exhibit non-monotonic trends in *Empirical L1 Error*, initially decreasing but later increasing during training, indicating overfitting to the limited known regions.

In contrast, TD-GFN consistently converges toward the target distribution throughout training. Owing to the strong generalization capabilities of the learned edge rewards, it avoids overfitting to the dataset and quickly identifies high-reward modes. These results highlight TD-GFN’s ability to maintain a favorable balance between exploration and exploitation, even under severely constrained data conditions.

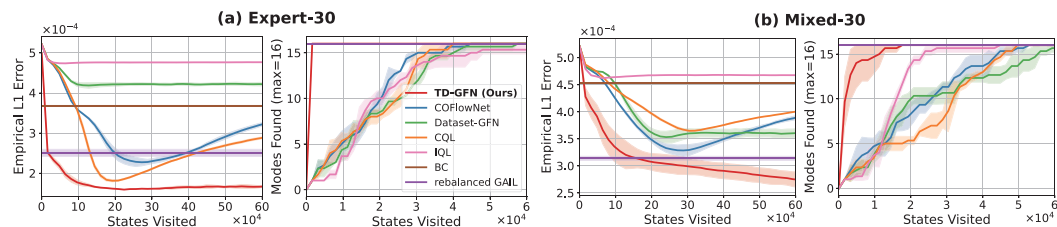


Figure 7: Performance comparison on the 8^4 Hypergrid task using 30 trajectories from the *Expert* and *Mixed* datasets.

D.2 Algorithm Visualization on Hypergrid

We visualize the behavior of our proposed TD-GFN in an 8×8 Hypergrid environment using a dataset comprising 400 transitions, constructed by combining trajectories collected from an expert policy (50%) and a random policy (50%). The edge rewards learned via IRL using Algorithm 2 are shown in Figure 8(b). Compared to the raw edge visitation frequencies from the dataset (Figure 8(a)), the learned edge rewards place greater emphasis on transitions that lead toward high-reward modes.

Notably, the learned edge rewards exhibit strong generalization: they assign meaningful values even to transitions that do not appear in the dataset (e.g., those in the topmost row), thereby guiding the policy toward out-of-distribution high-reward states, such as the modes in the top-right corner.

Figure 8(c) shows the pruned DAG based on the edge rewards in Figure 8(b). As illustrated, the resulting subgraph not only removes many transitions leading to low-reward regions—despite their presence in the dataset—but also constructs clear pathways toward high-reward modes, even when such paths were never encountered during data collection.

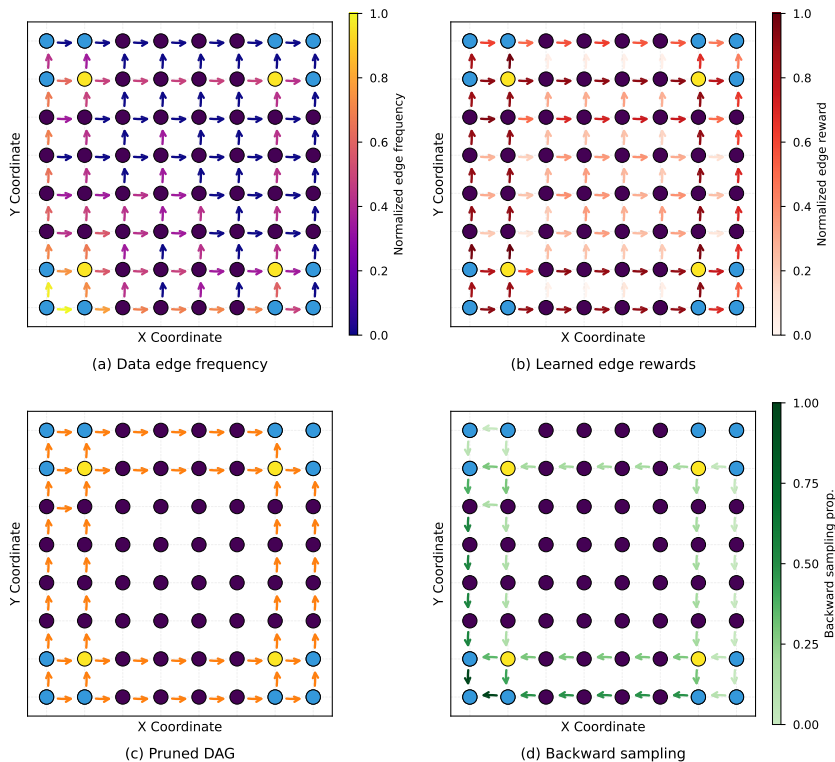


Figure 8: Visualization of TD-GFN in the 8×8 Hypergrid environment. (a) Normalized edge visitation frequencies in a dataset composed of 400 transitions obtained by combining trajectories collected separately from an expert policy (50%) and a random policy (50%); (b) Edge rewards learned via inverse reinforcement learning (IRL); (c) The pruned sub-DAG consisting of high-reward edges (highlighted in yellow) based on edge rewards; (d) The sampling probability of edges under backward policy induced by edge rewards and object rewards.

D.3 Time consumption and resource usage

For the Molecule Design task (Section 4.3), all algorithms are trained on an NVIDIA Tesla A100 80GB GPU. We report preprocessing time, per-epoch training time, total convergence time, and peak GPU memory usage for various GFlowNet training methods in Table 4.

For Proxy-GFN, preprocessing refers to training the proxy model. For COFlowNet, it involves constructing a dictionary that indexes all child nodes from the dataset for each state. For TD-

GFN, preprocessing includes both learning the edge rewards and pruning the environment DAG, corresponding to Phase 1 and Phase 2 in Algorithm 1.

Table 4: Training time and GPU memory usage comparison across GFlowNet variants on the Molecule Design task.

Method	Preprocessing Time	Epoch Time	Convergence Time	GPU Memory
Proxy-GFN	10h	4.82s	4h	22.88G
Dataset-GFN	/	0.56s	0.47h	10.08G
FM-COFlowNet	2h	0.76s	0.63h	12.81G
QM-COFlowNet	2h	1.16s	0.71h	63.80G
TD-GFN (Ours)	0.1h	0.59s	0.20h	12.01G

As shown, by predicting pruned edges through a single forward pass of a neural network—rather than querying from a pre-constructed dictionary—TD-GFN significantly reduces preprocessing time and incurs minimal computational overhead during training. Furthermore, owing to its rapid convergence (as demonstrated in Table 1), TD-GFN can learn a high-performing GFlowNet policy in under 30 minutes, highlighting its strong time efficiency.

Although the edge reward learning component introduces a modest computational cost, it remains negligible compared to the overhead of more complex mechanisms such as quantile matching. Despite this, TD-GFN outperforms methods enhanced with quantile-based techniques, underscoring its effectiveness and scalability.

D.4 Ablation Study

In this section, we conduct ablation experiments on the 8^4 Hypergrid task to evaluate the contribution of individual components within the proposed TD-GFN framework.

Dataset Rebalancing. As described in Section 3.1, we perform dataset rebalancing to adjust the offline data distribution to better approximate that of an expert policy. In Figure 9, we evaluate TD-GFN with and without rebalancing on both the *Expert* and *Bad* datasets. For additional comparison, we also train the offline GFlowNet method COFlowNet on the rebalanced datasets.

The results show that rebalancing the *Expert* dataset does not degrade policy learning, despite the mild distortion introduced to the original data distribution. More importantly, rebalancing significantly improves policy performance when the dataset is collected under a behavior policy that diverges substantially from the expert.

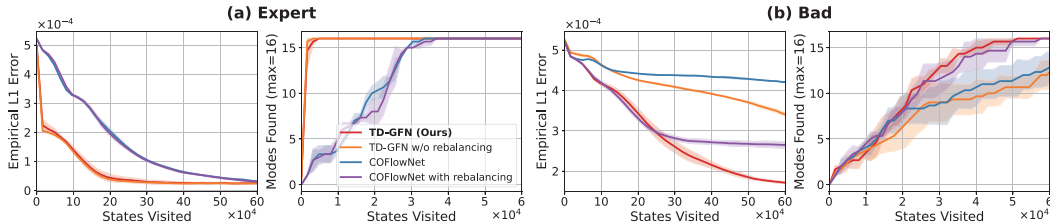


Figure 9: Performance comparison with and without dataset rebalancing on *Expert* and *Bad* datasets, each consisting of 1, 500 trajectories.

Pruning and Backward Sampling. To assess the individual impact of TD-GFN’s components, we conduct ablations on the *Mixed* dataset. We compare the full TD-GFN with three variants: (i) a baseline without DAG pruning; (ii) a dataset-pruned variant that removes all edges not observed in the dataset; and (iii) a backward sampling baseline in which trajectories are sampled uniformly in reverse from terminal nodes, without using learned edge rewards. As shown in Figure 10, both the reward-guided pruning strategy and the prioritized backward sampling procedure are critical to the overall performance of TD-GFN.

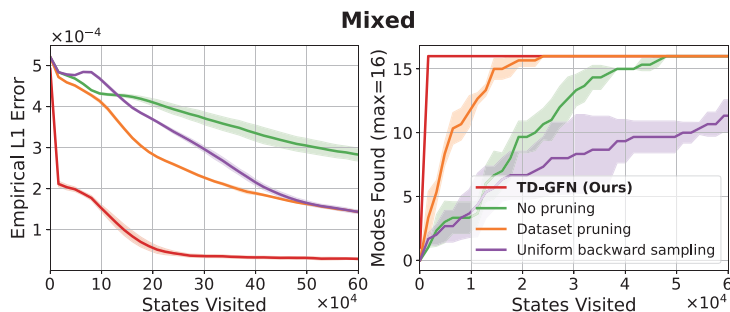


Figure 10: Ablation study on the *Mixed* dataset. We evaluate three TD-GFN variants: (i) no pruning; (ii) dataset-based pruning that removes unseen edges; and (iii) uniform backward sampling from terminal nodes. Each TD-GFN component proves essential for achieving optimal performance.

D.5 Orthogonality to Training Paradigms

As shown in Algorithm 1, the improvements introduced by TD-GFN are orthogonal to the specific training paradigm employed after trajectory collection. While we adopt the Flow-Matching (FM) objective [1] in this work, our framework is also compatible with alternative GFlowNet training objectives—such as DB [2], TB [42], and SubTB [48]—without requiring substantial modification.

Due to time and space constraints, we focus our empirical analysis on the integration of TD-GFN with offline RL methods and the quantile matching technique proposed in [38].

Replacing Flow Matching with Offline RL Training Instead of using the standard flow-matching objective in GFlowNet training, we examine the effect of replacing it with the Conservative Q-Learning (CQL) objective from offline reinforcement learning [35], resulting in a variant we refer to as TD-CQL. We evaluate TD-CQL on both the *Expert* and *Mixed* datasets, each consisting of 1, 500 trajectories. Results are presented in Figure 11.

With training components inherited from TD-GFN, TD-CQL successfully discovers all modes using a comparable number of state visits and achieves an *Empirical L1 Error* below 10^{-4} with fewer visits than TD-GFN, demonstrating strong sample efficiency and early-stage accuracy in modeling the target distribution. However, beyond this point, the *Empirical L1 Error* increases, indicating a decline in distributional approximation quality. This degradation arises from the nature of the offline RL objective, which tends to overfit the policy toward only the highest-reward objects, thereby limiting its ability to accurately model the full reward distribution.

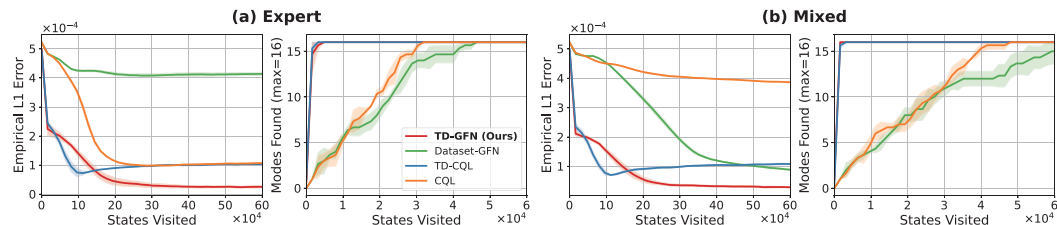


Figure 11: Performance comparison of TD-CQL on the *Expert* and *Mixed* datasets, each consisting of 1, 500 trajectories.

Incorporating Quantile Matching Following the approach of [22], we augment TD-GFN with the quantile matching technique proposed in [38], resulting in a variant referred to as QM-TD-GFN. We evaluate QM-TD-GFN on the Molecule Design task (Section 4.3) to assess its impact on the diversity of generated samples.

We observe that incorporating quantile matching into TD-GFN introduces significant training instability. This may be due to the pruned structure of the environment DAG, which reduces the need for a

highly uncertain policy. Nevertheless, in cases where training remains stable, QM-TD-GFN is able to discover more high-reward modes than the original TD-GFN, as shown in Figure 12. These findings highlight the potential of quantile matching to enhance the diversity of generated molecules.

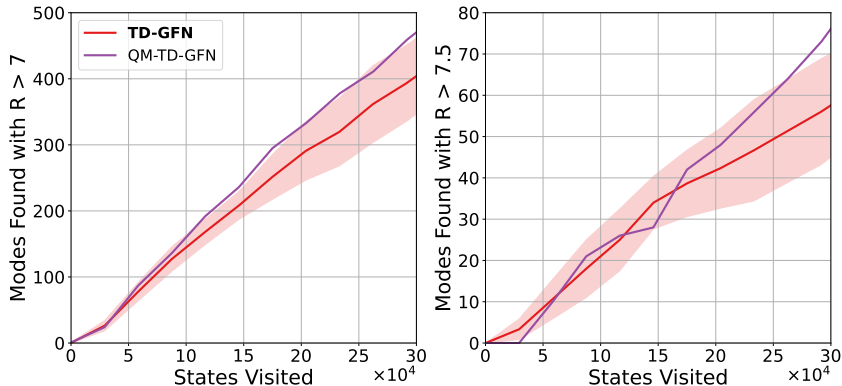


Figure 12: Number of high-reward modes discovered by QM-TD-GFN compared to TD-GFN.

D.6 Discussion on Baseline Performance

To gain deeper insight into the behavior of baseline methods, we analyze results on the Hypergrid task, as shown in Figure 13.

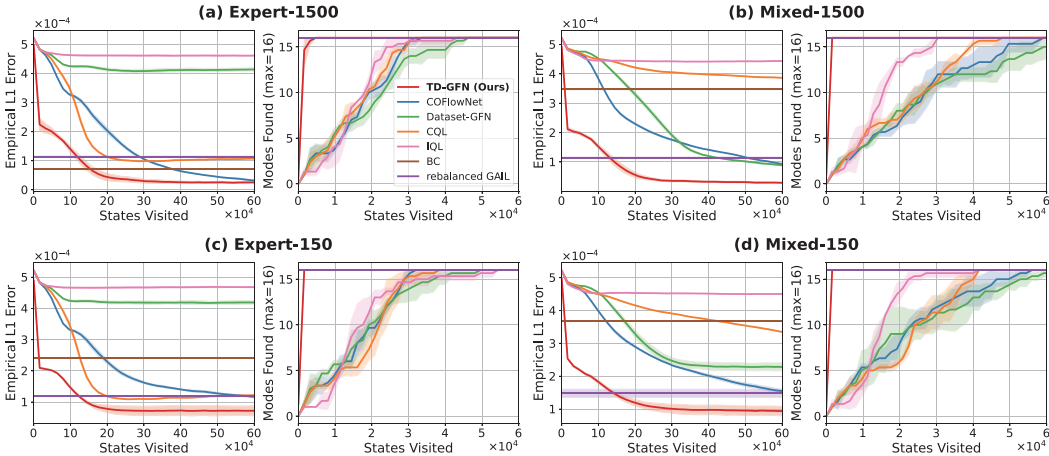


Figure 13: Performance comparison on the 8^4 Hypergrid task. The top row uses 1,500 trajectories from the *Expert* and *Mixed* datasets for policy training, while the bottom row uses only 150 trajectories.

Across datasets with varying levels of uncertainty, IQL excels at identifying high-reward modes. However, it also exhibits the highest *Empirical L1 Error*, underscoring a core characteristic of offline reinforcement learning algorithms: their objective often prioritizes recovering the most rewarding trajectories over accurately modeling the full reward distribution.

Although CQL is also an offline RL algorithm, its performance differs from IQL due to a distinct training paradigm. Unlike IQL, which learns exclusively from transitions in the dataset, CQL explicitly constrains policy actions to regions supported by the dataset by penalizing overestimation of Q-values. As a result, its performance is highly sensitive to dataset quality. A similar sensitivity is observed in COFlowNet, which applies conservative regularization to restrict the policy’s behavior to the data distribution’s support.

In contrast, GAIL—when trained on a rebalanced dataset—demonstrates stable performance across datasets. It consistently maintains coverage over all modes and achieves an *Empirical L1 Error* slightly above 1×10^{-4} . Although GAIL performs slightly worse than Behavior Cloning (BC) in scenarios with abundant expert data, it significantly outperforms BC under noisy or sparse data conditions and achieves performance comparable to COFlowNet. These results highlight the benefit of incorporating reward signals from terminal states during training by rebalancing the dataset.

E Future Directions

While TD-GFN demonstrates strong empirical performance and improved robustness over existing GFlowNet training methods, several limitations remain, suggesting promising directions for future research.

First, TD-GFN relies on an adversarial approach to estimate edge-level rewards, which can introduce training instability and requires careful hyperparameter tuning. Developing more stable and generalizable techniques for edge reward estimation—potentially drawing on recent advances in inverse reinforcement learning—could enhance the reliability and scalability of the framework.

Second, the current formulation of TD-GFN assumes a deterministic environment. Extending the method to accommodate stochastic rewards or non-deterministic transitions [56] is a critical direction, particularly for real-world applications where uncertainty is inherent in both reward evaluation and environment dynamics.